

About the impact of baryons on the cluster mass function: Fitting formula and cosmological implications

Sebastian, Alex, Klaus and whoever is interested

23 October 2014

ABSTRACT

Galaxy cluster surveys allow to place tight constraints on key cosmological parameters and to improve our knowledge about dark energy. In order to fully exploit current and next-generation cluster samples it is of crucial importance to rely on an accurately calibrated cluster mass function. Typically, the calibration is done against large N -body simulations, taking only dark matter into account. We use the hydrodynamical Magneticum simulations to quantify the impact baryons have on the cluster mass function. Including baryonic effects leads to...

Key words: cosmology: theory - cosmology: cosmological parameters

1 INTRODUCTION

240.0pt

504.0pt

Galaxy clusters are the largest collapsed objects in the Universe. Their distribution in mass and redshift is highly sensitive to key cosmological parameters such as the matter density Ω_m , or the amount of matter fluctuations in the Universe σ_8 . Furthermore, they can be used to constrain different models of dark energy as well the neutrino sector. Large cluster surveys have therefore proven as useful cosmological probes (e.g. Vikhlinin et al. 2009; Mantz et al. 2010; Rozo et al. 2010; et al. 2013; Planck Collaboration et al. 2013; Bocquet et al. 2014).

In all these analyses, the observed abundance of galaxy clusters is linked to the linear matter power spectrum through the cluster mass function, which can be estimated through an analytical approach (Press & Schechter 1974) or calibrated against numerical simulations. Tinker et al. (2008) use a set of large N -body simulations to provide a calibrated fitting function. While their mass function has established as the standard reference which is used in most cosmological analyses, the literature offers several alternatives (e.g. Jenkins et al. 2001; White et al. 2002; Warren et al. 2006; Watson et al. 2013). All these mass functions are comparable, and Planck Collaboration et al. (2013) show that their cosmological constraints are basically insensitive to the adopted mass function.

However, all mass functions obtained from N -body simulations suffer from the simplification of neglecting the baryonic component of the clusters. The pressure in the baryonic gas effectively leads to lower-mass clusters, and a decrease of the expected cluster abundance. Recently, various authors have investigated the baryonic impact on the cluster mass function (e.g. Cusworth et al. 2014). However, many of these works suffer from too simplistic modeling of the baryonic gas in the numerical simulations. Some of these simplifications are pre-heating at high redshift, negligence of radiative cooling or the baryons' self-gravity, and many other

(probably cite something). Nevertheless, these studies suggest that baryonic dynamics do have an appreciable impact on the cluster mass function, by lowering the overall abundance of clusters by about 15% Cusworth et al. (2014).

In this work, we analyze a simulated cluster sample generated by the Magneticum simulations (Dolag K. et al. 2014). These are a set of hydrodynamical simulations covering large cosmological volumes for a variety of resolutions. We use these data to calibrate a cluster mass function that takes into account baryonic effects. This paper is organized as follows: In Section 2 we present the Magneticum simulations and the cluster sample used for this work. In Section 3 we introduce our analysis method used to perform the fit, and show how we tested it for potential biases. We present our results in Section 4 and provide further discussion in Section 5.

2 SIMULATIONS AND CLUSTER SELECTION

2.1 The Magneticum Simulations

This Section will need some input from Klaus. Introduce the hydro sims and tell why they are so incredibly awesome. We also ran some DM simulations for comparison.

All simulations are carried out assuming a spatially flat Λ CDM cosmology with matter density $\Omega_m = 0.272$, baryon density $\Omega_b = 0.0456$, variance in the matter field¹ $\sigma_8 = 0.809$, and Hubble constant $H_0 = 70.4$.

2.2 Halo Selection

This Section needs input from Alex who actually produced the catalogs. Also mention that we chose a rather large number of particles

¹ See Equation 2 for the exact definition

2 Whoever is interested

Table 1. Mass function parameters from our dark matter simulations and hydro simulations for cluster masses defined as $M_{200,\text{mean}}$. The covariance matrices are presented in Table 2.

Parameter	A	a	b	c	A_z	a_z	b_z
DM	0.223 ± 0.024	1.69 ± 0.10	2.05 ± 0.23	1.242 ± 0.028	-0.25 ± 0.35	0.091 ± 0.088	-0.02 ± 0.31
hydro	0.282 ± 0.035	2.14 ± 0.18	1.54 ± 0.14	1.319 ± 0.039	-0.38 ± 0.33	0.022 ± 0.072	0.08 ± 0.21
Tinker et al. (2008)	0.186	1.47	2.57	1.19	-0.14	-0.06	0.011

for the haloes in the hydro simulations. Not sure if we explicitly mention the convergence problems we observed otherwise.

3 ANALYSIS METHOD

We provide the theoretical background on the cluster mass function and introduce its functional form. We then present the method used to perform the multi-dimensional fits used to extract the mass function parameters from our simulations.

3.1 The Cluster Mass Function

The number density of galaxy clusters with respect to mass is

$$\frac{dn}{dM} = f(\sigma) \frac{\bar{\rho}_m}{M} \frac{d \ln \sigma^{-1}}{dM}, \quad (1)$$

with the mean matter density $\bar{\rho}_m$ (at redshift $z = 0$) and the variance

$$\sigma(M, z) = \frac{1}{2\pi^2} \int P(k, z) \hat{W}^2(kR) k^2 dk \quad (2)$$

of the matter density field $P(k, z)$ smoothed with the Fourier transform \hat{W} of the real-space top-hat window function of radius $R = (3M/4\pi\bar{\rho}_m)^{1/3}$. The function $f(\sigma)$ is assumed to be independent of cosmology and is commonly parametrized as

$$f(\sigma) = A \left[\left(\frac{\sigma}{b} \right)^{-a} + 1 \right] \exp \left(-\frac{c}{\sigma^2} \right) \quad (3)$$

with four parameters A, a, b, c that need to be calibrated. Here, A sets the overall normalization, a and b are the slope and normalization of the low-mass power law, and c sets the scale of the high-mass exponential cutoff (analogous to e.g. Tinker et al. 2008).

The parameters will in general depend on redshift, and we adopt the parametrization as a power law of $1 + z$:

$$A(z) = A_0(1+z)^{-A_z} \quad (4)$$

$$a(z) = a_0(1+z)^{-a_z} \quad (5)$$

$$b(z) = b_0(1+z)^{-b_z} \quad (6)$$

where the subscript 0 denotes the values at redshift $z = 0$, and where A_z, a_z, b_z are additional fit parameters. The cutoff scale c is assumed constant as a function of redshift. Note that the cluster number density depends on redshift through $\sigma(M, z)$ and the explicit redshift dependence of $f(\sigma)$.

3.2 Parameter Estimation

When fitting for the mass function, we are facing a problem with moderately large dimensionality (7 parameters) and utilize the `emcee`² code for efficient exploration of parameter space

(Foreman-Mackey et al. 2013). The likelihood of each point in parameter space \mathbf{p} is calculated in the following way: We calculate the matter power spectrum using the transfer function by Eisenstein & Hu (1998, 1999) as this is the prescription used to set up the initial conditions of the Magneticum simulations. Then, for each redshift, we calculate the mass function following Equations 1-3. We apply a binning to the data that is equally distributed in log-space with $\Delta \log_{10} M = 0.01$. We checked that decreasing the bin size does not change our results. Finally, we evaluate the likelihood \mathcal{L} by applying the Cash statistics (Cash 1979), which is an application of Poisson statistics

$$\ln \mathcal{L} = \sum_i \ln \frac{dn(M_i|\mathbf{p}, z)}{d \log M} \Delta \log M - \int \frac{dn(M|\mathbf{p}, z)}{dM} dM, \quad (7)$$

where i runs over all clusters in the sample. Note that the second term equals the total number of expected clusters.

In practice, given a set of fit parameters \mathbf{p} , we perform the above calculation for each snapshot redshift and for each of the simulation's boxes separately, sum the log-likelihoods, and return the result to `emcee`.

We tested our fitting procedure against several mock catalogs that contain a factor 100 times more clusters than our data. We recovered the input values within the uncertainties and conclude that our fitting method is unbiased to a level that is much smaller than the errors we report.

4 RESULTS

Figure 2 shows our main results. We show the data points for the DM and hydro simulations as well as our best fit mass functions for both sets of simulations. The DM simulations are in good agreement with the fitting formula by Tinker et al. (2008), while it is clear that the hydro simulations predict less massive clusters. For redshifts smaller than about 1, we expect about 10% less clusters from the hydro simulations. Note however that the error bars are quite large, and the 2σ regions shown in Figure 2 still overlap.

In Table 1 we present the fit parameters obtained from our DM and hydro mass functions. Masses are defined as $M_{200,m}$. The corresponding covariance matrices are presented in Table 2.

- Present the overall goodness of the fits (χ^2).
- Same thing for each redshift, i.e. test whether the redshift evolution is adequately parametrized.
- Extract fit parameters for $M_{500,c}$ as this is more useful for current SZ and X-ray surveys.

5 DISCUSSION

- Analyze some (mock?) data and quantify the shift in Ω_m - σ_8 space, as in Figure 1.
- Compare this shift to current (and future?) constraints.
- How does it affect the cluster vs. CMB tension?

² <http://dan.iel.fm/emcee/current>

Table 2. Covariance matrices corresponding to the mean values presented in Table 1. Actually, this is not very interesting for the paper, but it is for people wanting to use our mass function. We could put this in some website.

DM							
Param.	A	a	b	c	A_z	a_z	b_z
A	4.53×10^{-4}	1.18×10^{-3}	-4.03×10^{-3}	1.06×10^{-4}	-7.55×10^{-4}	-1.75×10^{-4}	7.20×10^{-4}
a		9.87×10^{-3}	-1.35×10^{-2}	2.08×10^{-3}	3.64×10^{-3}	2.38×10^{-4}	-2.25×10^{-3}
b			3.99×10^{-2}	-1.05×10^{-3}	-7.62×10^{-4}	2.59×10^{-3}	-2.23×10^{-3}
c				7.71×10^{-4}	-8.43×10^{-5}	7.71×10^{-4}	-4.18×10^{-4}
A_z					1.05×10^{-1}	1.24×10^{-2}	-8.65×10^{-2}
a_z						6.43×10^{-3}	-1.46×10^{-2}
b_z							7.60×10^{-2}

Hydro simulation (This is just a placeholder, need to fill in the correct data!)							
Param.	A	a	b	c	A_z	a_z	b_z
A	4.53×10^{-4}	1.18×10^{-3}	-4.03×10^{-3}	1.06×10^{-4}	-7.55×10^{-4}	-1.75×10^{-4}	7.20×10^{-4}
a		9.87×10^{-3}	-1.35×10^{-2}	2.08×10^{-3}	3.64×10^{-3}	2.38×10^{-4}	-2.25×10^{-3}
b			3.99×10^{-2}	-1.05×10^{-3}	-7.62×10^{-4}	2.59×10^{-3}	-2.23×10^{-3}
c				7.71×10^{-4}	-8.43×10^{-5}	7.71×10^{-4}	-4.18×10^{-4}
A_z					1.05×10^{-1}	1.24×10^{-2}	-8.65×10^{-2}
a_z						6.43×10^{-3}	-1.46×10^{-2}
b_z							7.60×10^{-2}

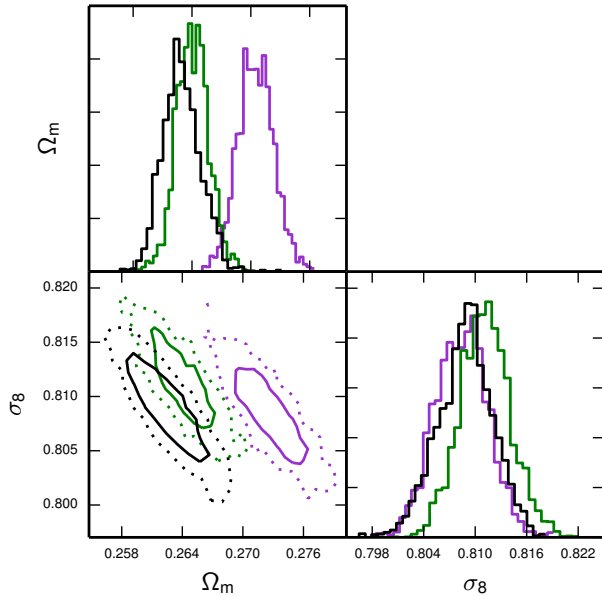


Figure 1. Likelihood contours (68% and 95% confidence) in Ω_m - σ_8 space for the cluster sample extracted from our hydro simulation. We analysed the sample using the Tinker et al. (2008) mass function (black), the mass function parameters obtained from our DM simulations (green) and from our hydro simulations (purple).

6 SUMMARY

Review our results. Point out that these kind of studies are crucial for the next-generation cluster surveys.

ACKNOWLEDGMENTS

We acknowledge the support of the DFG Cluster of Excellence ‘‘Origin and Structure of the Universe’’ and the Transregio program TR33 ‘‘The Dark Universe’’.

REFERENCES

- Bocquet et al. 2014, ArXiv e-prints
 Cash W., 1979, ApJ, 228, 939
 Cusworth S. J., Kay S. T., Battye R. A., Thomas P. A., 2014, MNRAS, 439, 2485
 Dolag K. et al. 2014, In Preparation
 Eisenstein D. J., Hu W., 1998, ApJ, 496, 605
 Eisenstein D. J., Hu W., 1999, ApJ, 511, 5
 et al. B., 2013, ApJ, 763, 147
 Foreman-Mackey D., Hogg D. W., Lang D., Goodman J., 2013, PASP, 125, 306
 Jenkins A., Frenk C. S., White S. D. M., Colberg J. M., Cole S., Evrard A. E., Couchman H. M. P., Yoshida N., 2001, MNRAS, 321, 372
 Mantz A., Allen S. W., Ebeling H., Rapetti D., Drlica-Wagner A., 2010, MNRAS, 406, 1773
 Planck Collaboration Ade P. A. R., et al. 2013, ArXiv e-prints
 Press W., Schechter P., 1974, ApJ, 187, 425
 Rozo E., Wechsler R. H., Rykoff E. S., Annis J. T., Becker M. R., Evrard A. E., Frieman J. A., Hansen S. M., Hao J., Johnston D. E., Koester B. P., McKay T. A., Sheldon E. S., Weinberg D. H., 2010, ApJ, 708, 645
 Tinker et al. 2008, ApJ, 688, 709
 Vikhlinin A., Kravtsov A. V., Burenin R. A., Ebeling H., Forman W. R., Hornstrup A., Jones C., Murray S. S., Nagai D., Quintana H., Voevodkin A., 2009, ApJ, 692, 1060
 Warren M. S., Abazajian K., Holz D. E., Teodoro L., 2006, ApJ, 646, 881
 Watson W. A., Iliev I. T., D’Aloisio A., Knebe A., Shapiro P. R., Yepes G., 2013, MNRAS, 433, 1230
 White M., Hernquist L., Springel V., 2002, ApJ, 579, 16

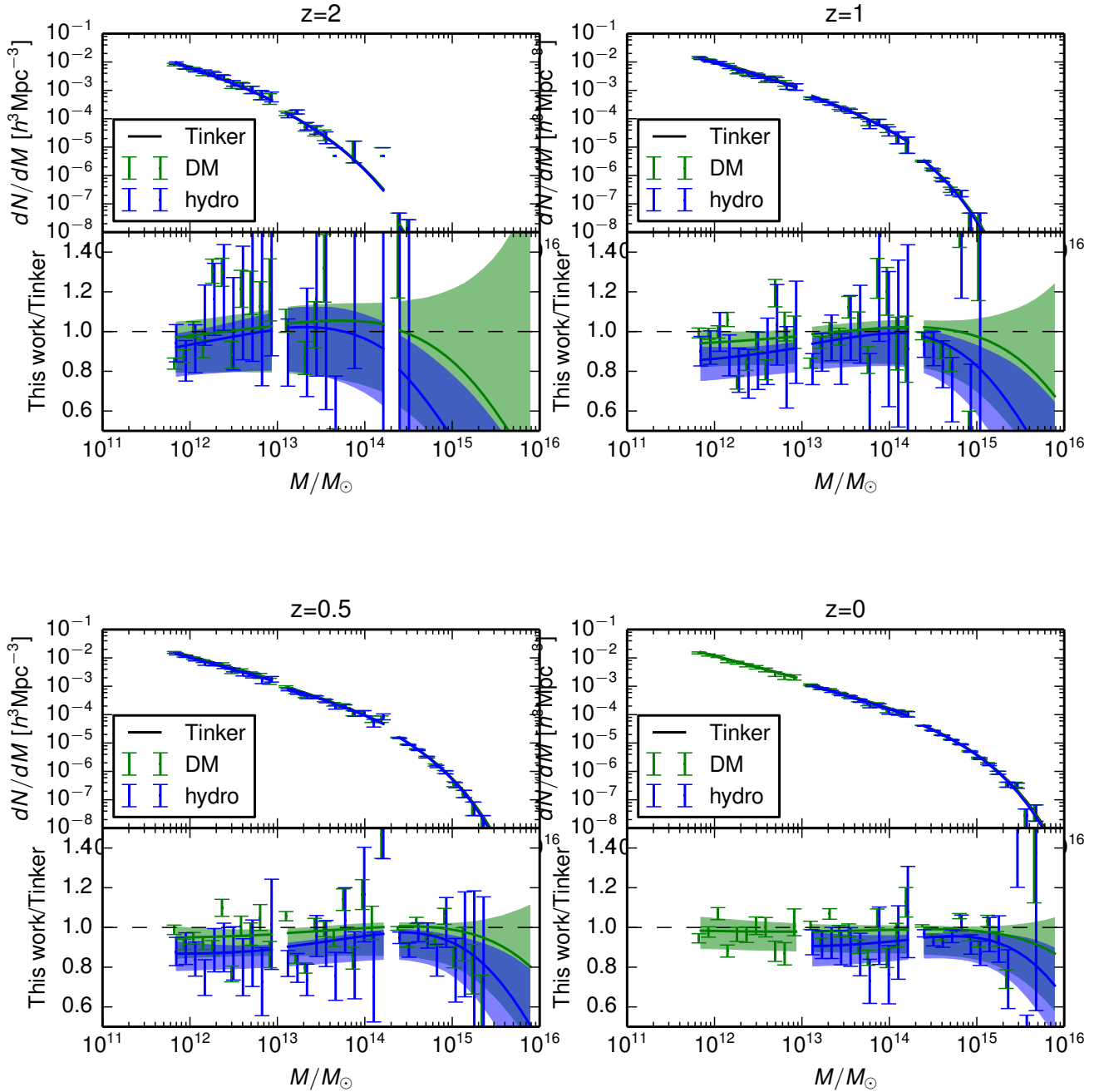


Figure 2. *Upper panels:* Mass function dN/dM obtained from our DM simulation (green) and our hydro simulation (blue) at four different redshifts. The fit from Tinker et al. (2008) is indicated by the black line. *Lower panels:* Relative difference between our simulations and the Tinker fit. The data points are slightly offset in mass direction for better readability. The solid lines correspond to the best fit; the colored regions correspond to the area enclosed within the 5th and 95th percentile (roughly the 2σ region).

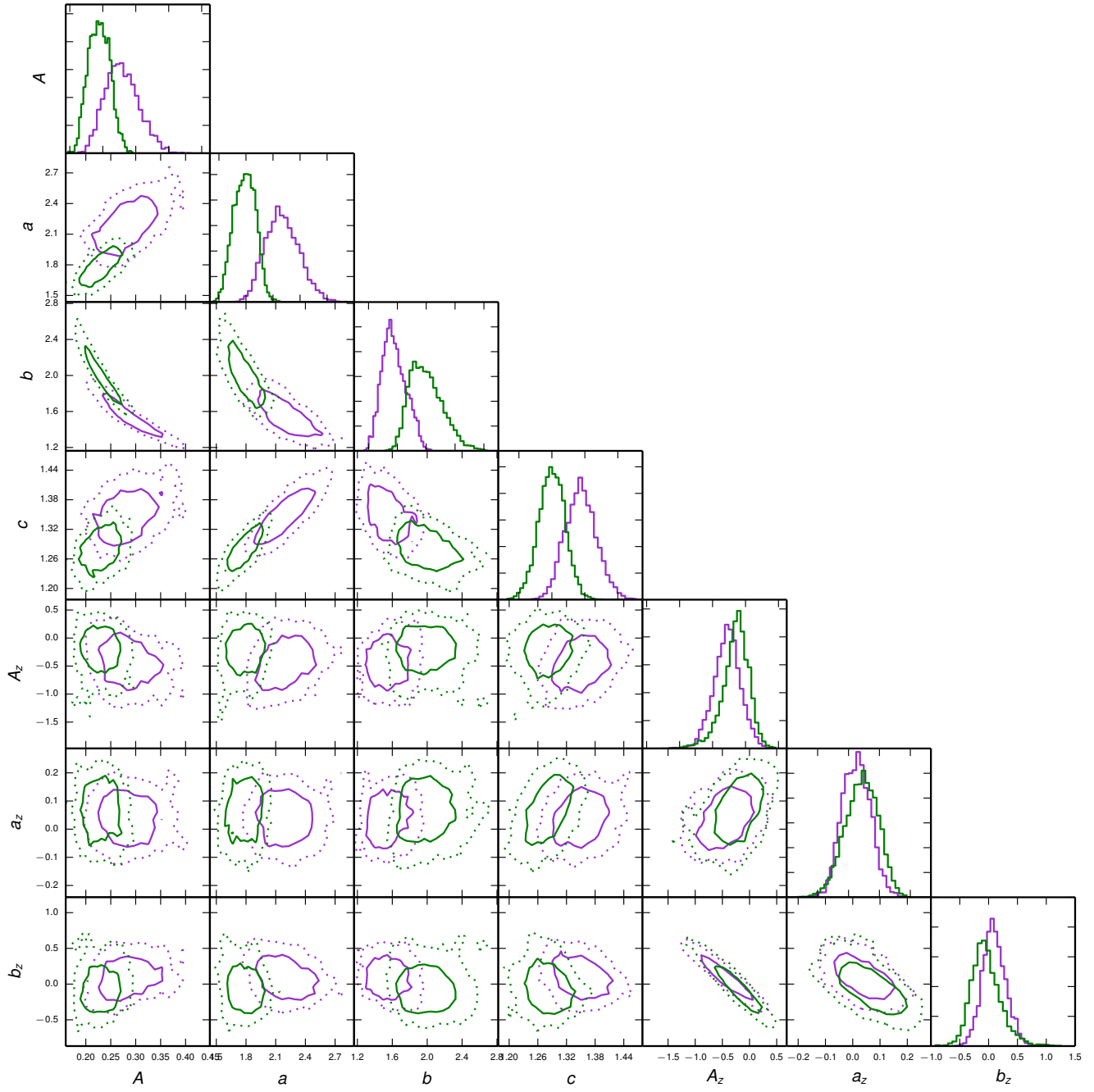


Figure 3. Parameter estimates for our dark matter simulation (green) and hydro simulation (blue).